JOURNAL OF ENVIRONMENTAL GEOGRAPHY
Journal of Environmental Geography 10 (3–4), 9–15.
DOI: 10.1515/jengeo-2017-0008
ISSN: 2060-467X

TOWARDS A CONTINUOUS INLAND EXCESS WATER FLOOD MONITORING SYSTEM BASED ON REMOTE SENSING DATA

Boudewijn van Leeuwen[1]*, Zalán Tobak[1], Ferenc Kovács[1], György Sipos[1]

[1]Department of Physical Geography and Geoinformatics, University of Szeged, Egyetem u. 2-6, H-6722 Szeged, Hungary
*Corresponding author, e-mail: leeuwen@geo.u-szeged.hu

Research article, received 3 October 2017, accepted 15 November 2017

Abstract

Inland excess water (IEW) is a type of flood where large flat inland areas are covered with water during a period of several weeks to months. The monitoring of these floods is needed to understand the extent and direction of development of the inundations and to mitigate their damage to the agricultural sector and build up infrastructure. Since IEW affects large areas, remote sensing data and methods are promising technologies to map these floods. This study presents the first results of a system that can monitor inland excess water over a large area with sufficient detail at a high interval and in a timely matter. The methodology is developed in such a way that only freely available satellite imagery is required and a map with known water bodies is needed to train the method to identify inundations. Minimal human interference is needed to generate the IEW maps. We will present a method describing three parallel workflows, each generating separate maps. The maps are combined to one weekly IEW map. At this moment, the method is capable of generating IEW maps for a region of over 8000 km^2, but it will be extended to cover the whole Great Hungarian Plain, and in the future, it can be extended to any area where a training water map can be created.

Keywords: inland excess water, Sentinel 1, Sentinel 2, monitoring, flood, water management

INTRODUCTION

Temporary inundations of large parts of the flat areas on the Great Hungarian Plain cause serious financial, environmental and social problems. On the contrary to riverine and coastal floods, these floods occur when – due to limited runoff, infiltration and evaporation – the superfluous water remains on the surface, or at places where groundwater – flowing towards lower areas – appears on the surface by leakage through porous soil. In literature, the inundations are often identified as inland excess water (IEW), surface ponding, areal flood or surface water flood (Rakonczai et al., 2011; Szatmári and van Leeuwen, 2013). Three main reasons can be identified to study IEW. It is studied to (1) understand the interrelated factors and processes that cause the formation of inland excess water, (2) to determine the location and size of the inundations to be able to take operative measurements to mitigate and prevent further damage, and (3) to forecast the location, size and duration of future floods to develop preventive policies (van Leeuwen et al., 2016).

Four general approaches have been applied to study the development, extent and duration of IEW inundations. First, in Hungary, since the second half of the 20th century, at national scale the extent of IEW was measured by observations in the field. These observations are labour intensive and therefore expensive. They are error prone due to differences in observation and interpretation techniques and they are usually performed infrequently, so they give an overview of the maximum extent of the flood, but it is not possible to use them for monitoring purposes. The second approach uses geographic information systems to combine many factors related to the development of IEW, to create maps describing the vulnerability of areas to the inundations. These maps are normally made at regional scale, which is the scale of most of the input data (Pálfai, 2003; Bozán et al., 2005; Bozán et al., 2009; Pásztor et al., 2014). Vulnerability maps provide information on the general probability that somewhere IEW will occur, but do not give information about the actual occurrences, nor about the development of the phenomenon. The third approach is the application of complex distributed models to simulate the hydrological processes causing IEW. Since this technique requires large amounts of very detailed input data, it is only feasible to use it at a small area. Depending on the quality of the input data, the technique can provide accurate information on the occurrence, extent and progress of IEW. It may also be able to forecast where IEW may occur (van Leeuwen et al., 2016). The last approach to the problem of IEW is the use of remote sensing data. In the past 30 years, studies have been published using aerial photographs (Licskó et al., 1987; Rakonczai et al., 2001; van Leeuwen et al., 2012), multispectral satellite data (Csornai et al., 2000; Rakonczai et al., 2001; Mucsi and Henits, 2010) and hyperspectral data (Csendes and Mucsi, 2016). Also, some experiments have been executed using active satellite data (Csornai et

al., 2000; Csekő, 2003; Gálya et al., 2016). The use of remote sensing techniques allows for the acquisition of data of medium (aerial photographs) to large areas (satellite data). Well understood processing techniques like classification and segmentation allow for the standardized processing of data and provide unified results over large areas. Common disadvantages of satellite data are their low temporal resolution and the limited availability of multispectral data due to bad atmospheric circumstances. Also, the resolution of non-commercial data was sometimes not suitable for IEW studies.

In 2014, as part of its Copernicus program, ESA started to launch the first satellites in its Sentinel Earth observation constellation (Malenovský et al., 2012). The data from the satellites is made publicly available free of charge and without restriction of use. With the formation of the Sentinel satellite constellations, to a large extent, the earlier disadvantages of satellite data can be overcome. For IEW monitoring, two types of satellites in the constellation are suitable. First, the Sentinel 1A and 1B satellites provide active remote sensing data with medium spatial resolution and a high temporal frequency. The active data is available under most weather conditions, and is therefore very suited for inland excess water monitoring. Second, Sentinel 2A and 2B provide multispectral data with a similarly high temporal and spatial resolution.

Contrary to earlier approaches, in this research, we developed a workflow that is capable of monitoring inland excess water on a weekly basis with sufficiently high resolution. The aim of the workflow is to produce IEW maps, that provide information on the location and extent of IEW for operational purposes, so operative measures can be initiated to mitigate and prevent further damage. The input data consists of a combination of Sentinel 1 radar images and Sentinel 2 or Landsat 8 multispectral images, complemented with a set of vector files providing a priori information about permanent water and other areas where inland excess water does not occur. All data is independently processed and combined at the end of the workflow to produce an integrated IEW map. For each IEW maintenance area, the relative coverage by inland excess water is calculated.

Many scientific publications have focused on causes of IEW, like soil characteristics (Barta, 2013; Gál and Farsang, 2013), land use (Barta et al., 2016), geomorphology (Benyhe and Kiss, 2012), or how they interrelate (e.g. Kozák, 2006; Rakonczai et al., 2011; Pásztor et al., 2014). Our approach concentrates on the continuous mapping of IEW for monitoring purposes and therefore factors related to the development of IEW are not taken into consideration.

STUDY AREA AND DATA

Study area

Due to its natural characteristics, inland excess water often occurs on the Great Hungarian Plain. Because of its low relief intensity combined with intensive or long periods of rainfall, mainly at the end of the winter, water does not run off to larger rivers nor infiltrates at a rate high enough to prevent it from remaining on the surface (Rakonczai et al. 2011). The southern region of the Great Hungarian Plain is maintained by the Lower-Tisza District Water Directorate and was selected as study area for this research (Fig. 1). It has a total area of almost 8200 km^2. The region is crossed by the Tisza and Maros rivers. Relief is limited to several meters of height difference and the lowest elevation in Hungary can also be found here. Based on its soil characteristics, the area can be divided in two parts; the western part has sandy soils, while the eastern part is covered with clay. The west is mildly sensitive to IEW according to the Palfai IEW Vulnerability map, while the east is moderately sensitive. Several disconnected areas are defined as highly vulnerable (Pálfai, 2003). The long-term average size of the area covered by the inundations in the study region is 10 800 ha per year. The largest area covered with IEW in recent times was 108 050 hectares in January 2000. The area is mainly agricultural, but there are also villages and some larger cities. The railroad and two highways have considerable influence on the development of inland excess water in the region (Barta et al., 2016).

Each of the used data sets covers the study area with one complete image or tile. The 175th ascending orbit of Sentinel 1 completely covers the area. Apart from a small strip in the west, the 34TDS Sentinel 2 tile covers the area, and the Landsat 8 WRS 187/28 covers the area except for a small area in the north. In this case study, the focus was to develop a method to generate inundation maps based on the individual images from different sources, therefore only the intersection of the footprints of the three satellite images was used to define the study area for this case study. This circumvents problems with mosaicking data of different acquisition times and sources.

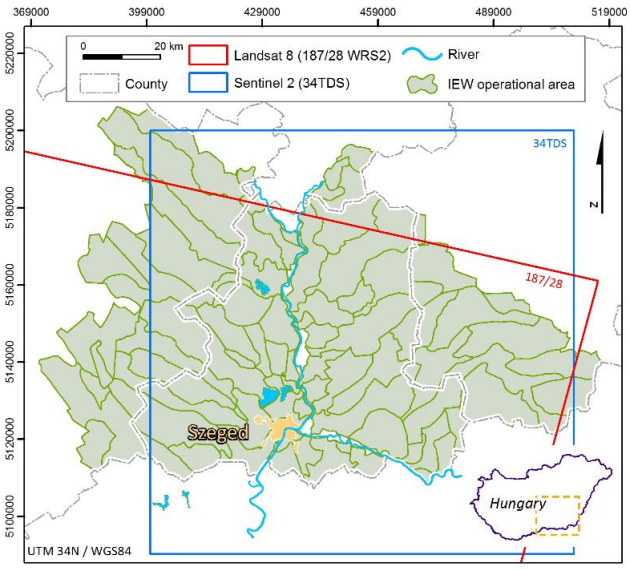

Fig. 1 The study area on the south part of the Great Hungarian Plain, showing the footprints of Sentinel 2 and Landsat 8 satellite imagery. Sentinel 1 covers the whole study area.

Data

Sentinel 1

The radar based part of the workflow uses data from the Sentinel 1A end Sentinel 1B satellites. The two satellites form a constellation that provides an image of the same area of Hungary about every third day, using identical instruments. Hungary is covered by 4 ascending and 4 descending paths (Fig. 2). In the presented workflow, we are using the Level-1 Ground Range Detected (GRD) product, that consists of focused SAR data that has been detected, multi-looked and projected to ground range using an Earth ellipsoid model. The phase information is lost. The product has approximately square resolution pixels and square pixel spacing with reduced speckle at the cost of reduced geometric resolution. Data was collected in the so-called Interferometric Wide (IW) swath mode and has a 250 km swath width and a pixel spacing of 10 x 10 meter (Malenovský et al., 2012). The data product comes with VV and VH polarization, which are both used in the workflow. Different objects in the terrain have different polarisation properties, therefor dual polarization images provide better options for object extraction. Sentinel 1 GRD IW data was used because it does not require further preprocessing, while it contains enough information to retrieve open water. The acquisition date of the analysed example image is 16 March 2016.

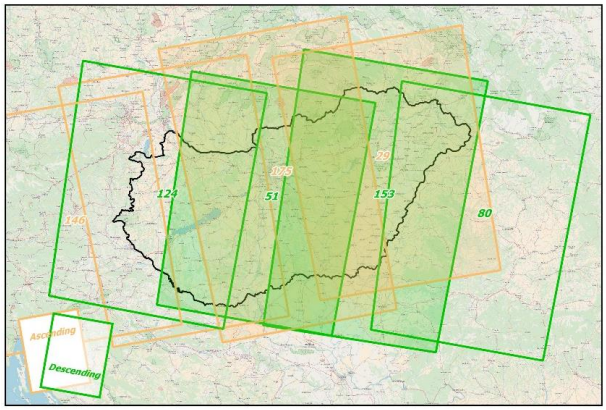

Fig. 2 Sentinel 1 paths covering Hungary

Sentinel 2

The ESA Copernicus program contains of two multispectral imaging satellites: Sentinel 2A and Sentinel 2B. At least once every 5 days, they provide high-resolution optical data in the visual, near infrared (NIR) and shortwave (SW) infrared spectral range for earth observation. Level 1C data products are tiled in 100x100 km tiles with 10 km overlap (Fig. 3) and store top-of-atmosphere reflectance values with UTM projection. Hungary is covered by 17 tiles in total. The applied visual and NIR bands have 10 meter spatial resolution, while the SW infrared bands have 20 meter spatial resolution. Data can be downloaded from Copernicus Open Access Hub in SAFE data package format. A cloud mask comes as metadata layer with every dataset. The study area is covered by the 34TDS tile. The acquisition date of the analysed example image is 21 March 2016.

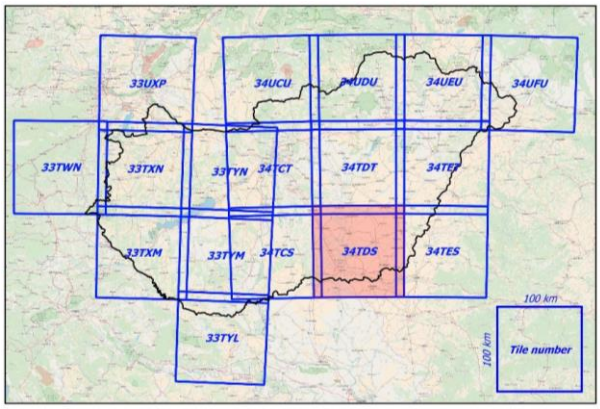

Fig. 3 Sentinel 2 tiles covering Hungary

Landsat

The Landsat OLI multispectral instrument acquires data in 9 spectral band between 0.43–2.4 μm with a temporal interval of 16 days. The 185x185 km images (Fig. 4) can be downloaded free of charge within 24 hours after their acquisition. The Landsat Surface Reflectance High Level Data Product "Surface Reflectance" L8SR data product provides 30 meter atmospherically corrected surface reflectance values for the first 7 spectral bands (USGS 2017). The data product also comes with a cloud mask identifying areas in the image that are not suitable for processing. The acquisition date of the analysed example image is 17 March 2016.

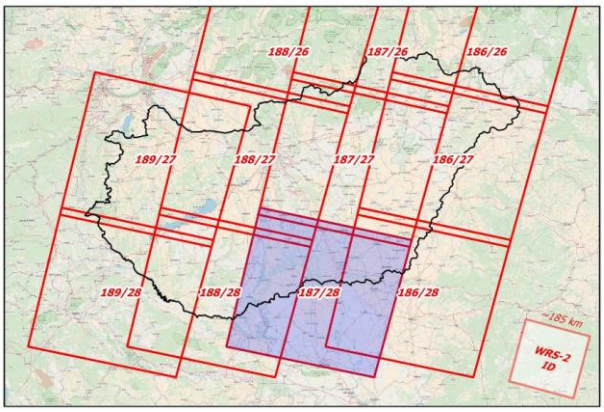

Fig. 4 Landsat 8 WRS paths covering Hungary

Auxiliary data

The active and passive remote sensing based workflows require a layer identifying open water. This file is necessary for the determination of the spectral thresholds and as training areas for the classification. Open water was extracted from the CORINE land cover 1:50 000 and 1:100 000 databases and the 20 meter Pan-European High Resolution Layers permanent water bodies maps (Copernicus HRL) (Büttner et al., 2014) and are stored in a vector layer. The open water file was updated by visually inspecting and editing differences using GeoEye imagery from 2014 - 2015 with a spatial resolution between 0.41 and 1.65 meter available in Google Earth. In this way, vegetation along the river banks, shadows and infrastructure in the water were removed from the open water layer.

Furthermore, urban areas, rural anthropogenic surfaces, paved roads and railroads were extracted from the CORINE databases and OpenStreetMap (OSM). These objects were stored in a mask layer, identifying areas that were excluded from the inland excess water calculations. The mask layer was further expanded with natural or man-made water bodies and wetlands. The floodplain between levees was also included in the mask.

The areas defined as cloud or cloud shadow in the Sentinel 2 and Landsat 8 cloud masks were not taken into considerations during the IEW calculations.

METHODS

The method proposed in this research is divided in workflows based on the type of input data. The active satellite data is used in a process where a threshold is defined to separate pixels with water and without water. The passive data sets are processed in two different ways. The first way uses unsupervised classification combined with an automatic method to select the water classes from the classification results. The second way is the calculation of a water index based on the ratios of bands. The following section describes each processing method in detail.

Downloading satellite data

All satellite data used in the workflow can be downloaded without restrictions and without charge. The Sentinel 1 and Sentinel 2 datasets can be downloaded manually from Copernicus Open Access Hub or in an automated way from API Hub using OpenSearch API and OpenData API. The downloaded product level is Level 1 GRD for Sentinel 1 and Level 1C for Sentinel 2 satellites. Raw Landsat 8 data can be downloaded from the USGS. To acquire Landsat surface reflectance data an on-demand request is required. This takes several days and may not always be suitable for operational purposes.

Preprocessing of satellite data and extraction of water surfaces

Radar data

A disadvantage of radar data is the complex geometric and radiometric processing required to extract useful information from the images. To start the extraction of the waterbodies, the Sentinel 1 data first needs to be radiometrically calibrated, a speckle filter needs to be applied to reduce the noise in the image, then the deformations due to the side looking geometry of the sensor and the terrain must be corrected, and finally a correction of the local incidence angle needs to be applied. After these initial steps, the data is geometrically and radiometrically corrected and transformed to a geometry that can be combined with the other data sets. The unit of the processed data is decibel (db).

In a geographic information system, the next steps are executed. First, the vector mask indicating the known open water is used to extract the statistics of water from the VV and VH radar images. The two sets of statistics are then used to extract similar pixels in the images, using a threshold method. The threshold method simply extracts pixels below a certain value (the maximum value in the reference statistics), presuming that the radar response of water is considerably lower than the response of other pixels. Some correction must be applied due to the statistics of outliers (which remained after the speckle filtering). In the final step of the radar processing workflow, those areas that are known as permanent water bodies or other none IEW areas are extracted from the map. The final map is a binary map with two classes: inland excess water inundations and other land cover.

Optical data

The downloaded Sentinel 2 and Landsat 8 datasets must be preprocessed before the interpretation of surface water patches is possible. The preprocessing workflow for optical data includes atmospheric correction which provides surface reflectance values; resampling of bands with a different pixel size to a common resolution; and spatial and spectral subsetting of the dataset to the study area and to the required spectral bands. To mask unusable areas covered by clouds or their shadow, auxiliary datasets have to be processed.

Unsupervised classification and class selection on optical data

The result of the applied classification algorithm must be evaluated using statistical methods to select the classes representing inundations. For this purpose, reference statistics must be created from training areas permanently or temporally covered by water. From the average of the reflectance values of the training pixels in each spectral band, a reference spectrum can be defined. After getting the reference spectra, the whole preprocessed image is classified. To support operative decisions an unsupervised clustering algorithm was selected to create a classified raster map and a signature file. The latter contains the statistical parameters - like minimum, maximum, mean, standard deviation in each band, and covariance matrix - of each cluster. In the last step, the spectral similarity between the reference class defined by the training areas and the individual clusters is evaluated. There are many different statistical methods to calculate spectral similarity or spectral separability between cluster of pixels in the n-D spectral space. Some of them, like for example Euclidean Distance use only the class mean values to measure n-D distances. Advanced calculations, like Divergence, Transformed Divergence and Jeffries-Matusita Distance (Swain and Davis, 1978), Bhattacharyya Distance (B-distance) (Jensen, 1986) use the covariance matrix beside the mean vector. In this research, the class similarity to the reference is calculated by the n-D Spectral Angle Difference method, which is not affected by the solar illumination factor and requires only the class means (Kruse et al., 1993). The result classes are rated based on this difference: a smaller angle means higher similarity and vice versa. Classes with the lowest spectral angle differences represent permanent water or inundations.

Spectral indices

In the infrared part of the electromagnetic spectrum, water is absorbed in the SWIR band, while reflected in the visible range. The Modified Normalized Differential Water Index (MNDWI, Xu 2005) uses the green and shortwave infrared bands from Sentinel 2 and Landsat 8 to extract open water according to the following expression:

$$\text{MNDWI} = \frac{\rho_{green} - \rho_{SWIR}}{\rho_{green} + \rho_{SWIR}} \quad \text{(Eq. 1)}$$

where ρ_{green} is band 3 for Sentinel 2 and Landsat 8 and ρ_{SWIR} is band 11 for Sentinel 2 and band 6 for Landsat 8

If the water content decreases, the reflectance in SWIR increases, resulting in a reduced value of the MNDWI index. Based on the MNDWI values calculated from the permanent open water zones in the open water mask, empirically threshold values were defined for the two indicators:

MNDWI (L8) >= -0,25 and MNDWI (S2) >= -0,35

Using these thresholds, a binary map was derived with two classes: inland excess water inundations and other land cover.

Integration

The maps that are created based on different input data and using different processing methods need to be integrated to one inland excess water map. For this case study, only images that cover the same area have been used. In the operative situation, this is not realistic since one satellite image does not cover the complete Great Hungarian Plain, and neighbouring images are collected on different dates. This results in a complex situation where output maps from different sources and different acquisition dates will need to be mosaiced.

RESULTS

In 2016, no exceptionally large amount of inland excess water occurred, but from half of February until half of March, some IEW developed in the study area. Using the described method IEW maps were created for this period (week 6 - week 11, 6 February - 18 March). As an example, figures 5 and 6 show the results for week 11 (13 – 19 March). In this week, all three sources of satellite data, Sentinel 1, Sentinel 2 and Landsat 8 were available. Figure 5 shows the results of the active data processing workflow, the unsupervised classification and the index based IEW identifications. Obviously, every method provides slightly different results. The largest difference is visible in the southeast quadrant where clouds and cloud shadows disturb the unsupervised classification result.

When the three workflows are combined, one IEW map is created. The different input maps are weighted to define the areas with the highest confidence that IEW indeed occurred at the indicated pixels. Figure 6 shows only those areas where inundations were identified using all three methods. Using data from 3 different sources (Sentinel 1, Sentinel 2 and Landsat 8) and using three different processing techniques (thresholding, unsupervised classification and indexing) results in maximum 5 separate IEW maps. If all 5 maps indicate IEW for a certain pixel, the change that IEW was indeed happening at that pixel is larger than when only one method identified IEW at that particular pixel. Combining the different maps and counting the amount of positive IEW identifications gives an indication for the confidence of IEW.

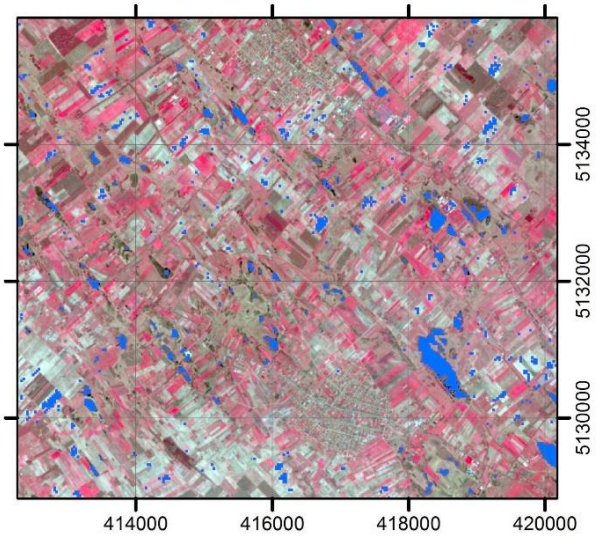

Fig. 6 The integrated inland excess water map based on three different sources/methods for week 11, 2016. Blue indicates water surface

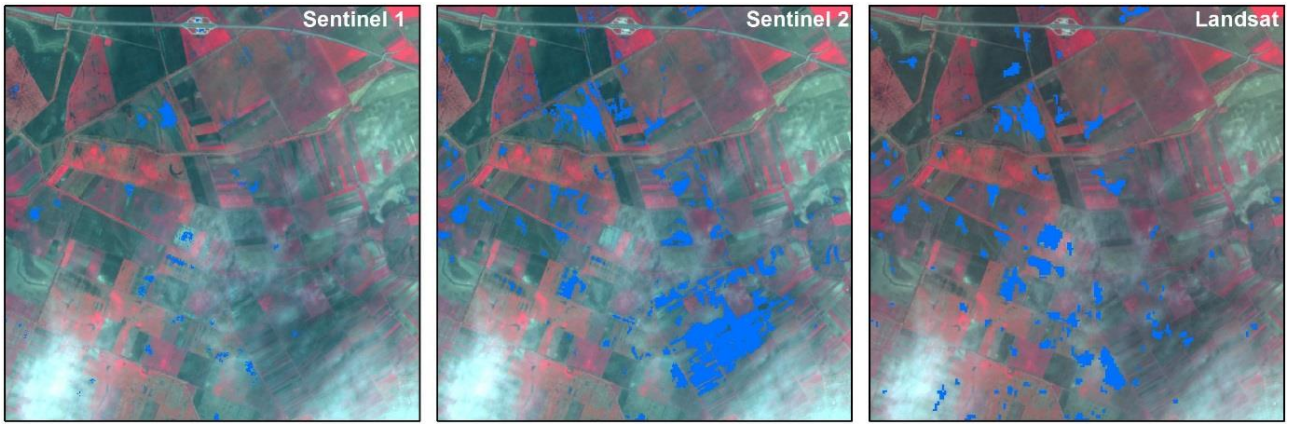

Fig. 5 Sentinel 2 false colour composite (RGB 843) covered with the results of the three separate processing workflows

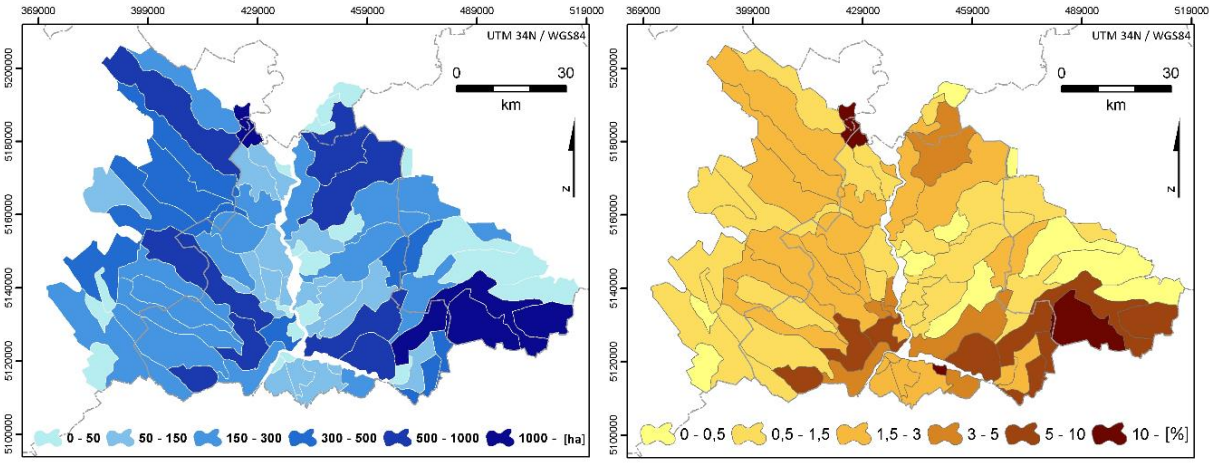

Fig. 7 Result maps showing the absolute (in hectare within the area) and relative (as percentage of the area) distribution of inland excess water per maintenance area in the Lower-Tisza District Water Directorate region

Based on the combined IEW maps, thematic maps are created indicating the area and ratio of IEW per IEW maintenance areas (Fig. 7). In operational circumstances, these maps can be used to determine spatial distribution of the severity of IEW throughout the region.

DISCUSSION

The presented method consists of three different workflows. Each workflow is aimed to create separate inland excess water maps based on procedures that can be used in an operational environment. Since the workflow has to be executed within a few days of the acquisition of the data, sometimes the proposed methods are a compromise between speed and accuracy. Deliberately, methods are developed that can be automated, so human influence is reduced to a minimum. This also means that there is no possibility for fine tuning of the method to specific situations. This may reduce the accuracy of the method.

The threshold method applied to the active data is a relatively simple method, that is easy to automate. In operative circumstances it provides reasonable results, but other techniques might be more suitable when performing detailed IEW studies at local scales. The speckle filtering is only based on a single image; therefore, it is not perfect and leaves unwanted spikes in the data which reduce the quality of the extracted statistics. Improvements in the speckle filtering should be investigated to improve the method. Another promising method is radar based change detection. This method might be useful to identify false positives resulting from the threshold method.

Inland excess water normally occurs during periods of bad weather and clouds. Our method uses multispectral satellite data to complement the active data, but the use of the multispectral data is often hampered due to clouds. Using a cloud mask allows us to use those parts of the multispectral data that are not covered by clouds. In the current method, standard cloud masks are used that come with the data products. These masks sometimes do not incorporate all clouds in the images and therefore sometimes lead to misclassifications. Improvements of the cloud mask can improve the multispectral data based inundation maps.

The result of earlier IEW research is often a single map that contains 4 classes: dry land, open water, saturated soil and vegetation in water. The presented workflow ignores the last two categories and therefore probably underestimates the total amount of inland excess water in the region. The determination of the last two categories requires additional data, which changes rapidly in space and time, and this makes it difficult, if not impossible to incorporate them in an automated operative environment, that produces timely, weekly inundation maps for large areas.

The intersection of the three data sources was used to determine the study area for this case study. Of course, in operational circumstances the complete Great Hungarian Plain needs to be used in the calculations. This increases the complexity of the method.

The method could be enhanced using other a priori data sets. The sandy soils show an overestimate of IEW inundations. This problem was reduced by applying a different threshold to the radar data, based on the soil type. Also, other errors or inconsistencies could be reduced by adding information on e.g. land cover or soil type and by building up a database of landcover dependent threshold values.

The proposed method can generate timely IEW maps for large areas. Independent cross validation of these maps is difficult because they cover large areas and other reliable data is not available. Visual inspection of the results using high resolution imagery of small areas indicate that the method identifies inundations at the proper locations. A larger validation campaign based on high resolution aerial photographs of large areas is needed and planned.

CONCLUSION

Earlier approaches to mapping inland excess water were based on field measurements or aerial or satellite remote sensing data for a specific date. We present a method that

is capable of continuously identifying inland excess water over large areas for operative purposes. It shows that combining the most recent active and passive data sources that are available at a very high temporal resolution provide new opportunities and challenges. The presented method provides maps that can be used by the Hungarian water directorates to mitigate damage caused by inland excess water, but there are still quite some problems and possibilities for improvements. More scientific research is needed to improve the determination of the threshold for the active data processing workflow and to reduce the number of false positives. Also cloud masking of the multispectral data can be improved to better select data suitable for processing. Finally, methods for mosaicking the different data from different acquisition dates within the operational workflow need to be developed.

ESA's Sentinel satellites will continue to provide base data to derive IEW maps, which allow for the development of a monitoring database. This database can be used to calculate frequency maps which indicate the vulnerability of an area to inland excess water.

Acknowledgements

This research was funded by the WATERatRISK project (HUSRB/1602/11/0057).

References

Barta, K. 2013. Inland Excess Water Projection Based on Meteorological and Pedological Monitoring Data on a Study Area Located in the Southern Part of the Great Hungarian Plain. *Journal of Environmental Geography* 6 (3-4), 31–37. DOI: 10.2478/jengeo-2013-0004

Barta, K., Szatmári, J., Posta, A. 2016. Connection Between Inland Excess Water Development and Motorways. *Carpathian Journal of Earth and Environmental Sciences* 11 (1), 293–301.

Benyhe, B., Kiss, T. 2012. Morphometric analysis of agricultural landforms in lowland ploughed fields using high resolution digital elevation models. *Carpathian Journal of Earth and Environmental Sciences* 7 (3), 71–78.

Bozán, Cs, Körösparti, J., Pásztor, L., Kuti, L., Kozák, P., Pálfai, I. 2009. GIS-based mapping of excess water inundation hazard in Csongrád county (Hungary). In.: Proceedings of the International Symposia on Risk Factors for Environment and Food Safety & Natural Resources and Sustainable Development, Faculty of Environmental Protection, November 6-7 Oradea, 678–684.

Bozán, Cs., Pálfai, I., Pásztor, L., Kozák, P., Körösparti, J. 2005. Mapping of Excess Water Hazard in Békés and Csongrád Counties of Hungary. In.: ICID 21st European Regional Conference Integrated Land and Water Resources Management: Towards Sustainable Rural Development, Frankfurt (an Oder) and Slubice, Germany and Poland, p.4

Büttner, G., Soukup, T., Kosztra, B. 2014. CLC2012 Addendum to CLC2006 Technical Guidelines. EEA, p.35.

Csekő, Á., 2003. Árvíz- és belvízfelmérés radar felvételekkel (Flood and inland excess water survey using radar imagery), *Geodézia és Kartográfia* 2, 16–22. (in Hungarian).

Csendes, B., Mucsi, L. 2016. Inland excess water mapping using hyperspectral imagery, *Geographica Pannonica* 20 (4), 191–196. DOI: 10.18421/GP20.04-01

Csornai, G., Lelkes, M., Nádor, G., Wirnhardt, Cs. 2000. Operatív árvíz- és belvíz-monitoring távérzékeléssel (Remote sensing based operative flood and inland excess water monitoring). *Geodézia és Kartográfia* 52 (5) 6–12. (in Hungarian).

Gál, N., Farsang, A. 2013. Weather extremities and soil processes impact of excess water on soil structure in the Southern Great Hungarian Plain, In: Lóczy D. (ed.) Geomorphological impacts of extreme weather: Case studies from Central and Eastern Europe. Springer, 313–325.

Gálya, B., Riczu, P., Blaskó, L., Tamás J. 2016. Belvíz érzékenység vizsgálata radar adatok alapján (Radar data based inland excess water sensitivity study), In: Az elmélet és a gyakorlat találkozása a térinformatikában VII. = Theory meets practice in GIS. Debrecen: Debreceni Egyetemi Kiadó, 161–168. (in Hungarian).

Jensen, J.R. 1986. Introduction Digital Image Processing. Prentice-Hall, Englewood Cliffs, New Jersey, 379 p.

Kozák, P. 2006. A belvízjárás összefüggéseinek vizsgálata az Alföld délkeleti részén, a vízgazdálkodás európai elvárásainak tükrében (The evaluation of the excess surface waters on the Hungarian lowland's south-east part, in the expectation of the water management in Europe), Doctoral Thesis, University of Szeged 103 p. (in Hungarian).

Kruse, F., Lefkoff, A.B., Boardman, J., Heidebrecht, K.B., Shapiro, A.T., Barloon, P.J., Goetz, A. 1993. The Spectral Image Processing System (SIPS)-Interactive Visualization and Analysis of Imaging Spectrometer Data. *Remote Sensing of Environment* 44. 145–163. DOI: 10.1016/0034-4257(93)90013-n

Licskó, B, Vekerdy, Z., Szilágyi, A., Busics, I., 1987. Távérzékelési módszertani útmutató a meliorációs tanulmánytervek készítéséhez (Handbook for remote sensing methodology for the preparation of land improvement plans), Földmérési és Távérzékelési Intézet, Budapest. (in Hungarian).

Malenovský, Z., Rott, H., Cihlar, J., Schaepman, M.E., García-Santos, G., Fernandes, R., Berger, M. 2012. Sentinels for science: Potential of Sentinel-1, -2, and -3 missions for scientific observations of ocean, cryosphere, and land. *Remote Sensing of Environment* 120, 91–101. DOI: 10.1016/j.rse.2011.09.026

Mucsi, L., Henits, L. 2010. Creating excess water inundation maps by sub-pixel classification of medium resolution satellite images. *Journal of Environmental Geography* 3 (1–4), 31–40.

Pálfai I., 2003. Magyarország belvíz-veszélyeztetettségi térképe (Hungarian inland excess water map). *Vízügyi közlemények* 85 (3), 510–524. (in Hungarian).

Pásztor, L., Körösparti, J., Bozán, Cs., Laborczi, A. & Takács, K. 2014. Spatial risk assessment of hydrological extremities: Inland excess water hazard, Szabolcs-Szatmár-Bereg County, Hungary. *Journal of Maps* 11 (4), 636–644. DOI: 10.1080/17445647.2014.954647

Rakonczai, J., Farsang, A., Mezősi, G., Gál, N. 2011. A belvízképződés elméleti háttere (Conceptual background to the formation of inland excess water). *Földrajzi Közlemények* 35 (4), 339–350. (in Hungarian).

Rakonczai, J., Mucsi, L., Szatmári, J., Kovács, F., Csató, Sz. 2001. A belvizes területek elhatárolásának módszertani lehetőségei (Methods for deliniation of inland excess water areas). In.: A földrajz eredményei az új évezred küszöbén. Az I. Magyar Földrajzi Konferencia CD kötete, SZTE TFGT, Szeged. p.14. (in Hungarian).

Swain, P. H., Davis, S.M. 1978. Remote Sensing: The Quantitative Approach, McGraw-Hill.

Szatmári, J., van Leeuwen, B. 2013. Inland Excess Water – Belvíz – Suvišne Unutrašnje Vode, Szeged; Újvidék: Szegedi Tudományegyetem; Újvidéki Egyetem, p.154.

USGS, 2017. LANDSAT 8 surface reflectance code (LaSRC) product. Ver.4.1. User guide, Department of the Interior, p.39.

van Leeuwen, B., Mezősi, G., Tobak, Z., Szatmári, J., Barta, K., 2012. Identification of inland excess water floodings using an artificial neural network. *Carpathian Journal of Earth and Environmental Sciences* 7 (4), 173–180.

van Leeuwen, B., Právetz, T., Liptay, Z.A., Tobak, Z. 2016. Physically based Hydrological Modelling of Inland Excess Water, Carpathian *Journal of Earth and Environmental Sciences* 11 (2), 497–510.

Xu, H., 2005. A study on information extraction of water body with the modified normalized difference water index (MNDWI), *International Journal of Remote Sensing* 5, 589-595. DOI: 10.1080/01431160600589179